International Journal of Pharmaceutics, 60 (1990) 11–26
Elsevier

IJP 02014

Physicochemical characterization of furosemide modifications

Yoshihisa Matsuda and Etsuko Tatsumi

Kobe Women's College of Pharmacy, Higashinada, Kobe 658 (Japan)

(Received 13 July 1989)
(Modified version received 25 September 1989)
(Accepted 13 October 1989)

Key words: Furosemide; Polymorphism; Crystal form; X-ray diffraction; Thermal analysis; Infrared spectroscopy; Solubility

Summary

The polymorphism of furosemide has been extensively investigated and characterized using X-ray powder diffractometry, differential scanning calorimetry, infrared and Fourier transform infrared spectroscopy, elemental analysis, hot-stage microscopy and scanning electron microscopy. Comparative analysis of the results reported by Doherty and York (1988) with the present data was performed to a high degree of precision in order to determine the points of agreement and difference between the two studies. The aforementioned authors investigated only two polymorphs (one stable and one metastable form), contrasting with our findings of five new types of modification (two polymorphs, two solvates and one amorphous form) in addition to the crystal forms. Among the seven modifications, enantiotropism was observed between two stable forms (low- and high-temperature-stable forms). On heating, the two metastable forms underwent transformation directly to the high-temperature-stable form whereas the situation in the case of the solvates involved progression via the intermediate stage of the low-temperature-stable form. The thermodynamic stability of these four polymorphs is discussed in relation to the activation energy and heat of transformation. A distinctly different degree of physicochemical photostability (coloration) was evident among the modifications; although the stable form did not show significant coloration even when irradiated with intense light, the other crystal forms were very susceptible to coloration. One of the metastable forms (form (III)) far surpassed any of the other crystal forms in dissolution properties.

Introduction

Furosemide is widely used as a diuretic or antihypertensive drug. It is also employed clinically as an important control for evaluating the therapeutic effect of a drug on renal insufficiency. Since this drug is practically insoluble in water, improvement of its dissolution properties is essential in view of the fact that the in vitro dissolution behavior of furosemide tablets is closely related to bioavailability (Kingsford et al., 1984; McNamara et al., 1987). Preparation of solid dispersions of the drug with water-soluble polymers, e.g., polyethylene glycol 6000 (Dubios and Ford, 1985), polyvinylpyrrolidone (Doherty and York, 1987a,b), or enteric coating agents (Hasegawa et al., 1985), represents an effective method for achieving better dissolution profiles, as the drug is dispersed in an amorphous state in such matrices. The thorough characterization of crystal forms of the drug is a matter of practical importance for achieving greater bioavailability and ensuring higher quality of dosage forms. We are aware of only a single report in the literature (Doherty and

Correspondence: Y. Matsuda, Kobe Women's College of Pharmacy, Higashinada, Kobe 658, Japan.

York, 1988) concerning the crystalline state of furosemide.

Part of our results on the polymorphism of the drug has been presented independently at both the 104th Annual Meeting of The Pharmaceutical Society of Japan in 1984 and the 7th Symposium on Development and Evaluation of Pharmaceutical Preparations held by the same Society in 1988 (Matsuda and Tatsumi, 1989). A thorough comparison of their data with ours revealed surprisingly many aspects of the methodology in common between both investigations. However, we noticed a number of discrepancies which present problems including that of the serious oversight of polymorphism in their reference data. While they described the polymorphism of only two crystal forms (forms I and II), we discovered six new forms of modification (three polymorphs, two solvates and one amorphous form) besides one crystal form of the drug which is manufactured commercially. The purpose of the present paper concerns the thorough elucidation of those aspects for which both studies accord and those which demonstrate disagreement, with particular emphasis on the benefits afforded by our innovation.

Materials and Methods

Preparation of modifications

A bulk sample of furosemide JP (lot no. 011557) was obtained from Shizuoka Caffeine Co. (Shizuoka, Japan). Six modifications of the drug were prepared using 18 kinds of solvents as described in Results and Discussion. To avoid confusion in the nomenclature of the polymorphs as prepared in the present article and as designated forms I and II in the paper of Doherty and York (1988), we distinguish our types of modifications by the addition of parentheses to the Roman numerals.

A brief outline of the preparative procedure is as follows:

Forms (I) and (II) A hot saturated solution of drug in methanol and a solution of the drug in *n*-butanol (forms (I) and (II), respectively) were allowed to stand at room temperature. The separated crystals were then filtered and dried in vacuo.

Form (III) An acetone solution of the drug (10 g/200 ml) was evaporated to dryness at 25 °C under reduced pressure in a rotary evaporator.

Form (IV) (dimethylformamide solvate) A small amount of water was added to a (DMF) solution of the drug (10 g/30 ml) with stirring until separation of crystals from the solution began, after which the crystals were filtered and dried.

Form (V) (dioxane solvate) A solution of the drug in 1,4-dioxane (10 g/300 ml) was evaporated to dryness at 50 °C in the same manner as for form (III).

Amorphous form The drug (0.5 g) was dissolved in 200 ml of a chloroform/methanol (4 : 1) cosolvent and the solution was fed into a mini-spray drier (model Mini-Spray h_0, Yamato Kagaku, Japan) through a peristaltic pump at a flow rate of 10 ml/min. The temperature at the inlet of the drying chamber of the apparatus was maintained at 40 °C. The yield of the sample recovered was approx. 20%.

X-ray powder diffraction analysis

Powder diffraction patterns were recorded on an X-ray diffractometer (Geigerflex 2011, Rigaku Denki, Japan) using Ni-filtered Cu-K_α radiation. The diffractograms were recorded under the following conditions: 35 kV, 7 mA, range 1000 cps, time constant 1 s, scan rate 4° 2θ/min, angular range 5–30° 2θ, divergence slit 1°, scatter slit 1°, receiving slit 0.15 mm.

Diffractograms for forms (I)–(III) at room and high temperatures were also recorded on another X-ray diffractometer equipped with a heating apparatus (model XD-610, Shimadzu, Japan) using the same radiation as for the above diffractometer. In this temperature-dependent method, sample scanning was limited to a range of 10–30° 2θ at a speed of 2° 2θ/min owing to the mechanical condition of the apparatus. Other conditions for operation were as follows: 40 kV, 25 mA, range 2000 cps, time constant 1 s, divergence slit 1°, scatter slit 1°, receiving slit 0.15 mm.

Thermal analysis

Differential scanning calorimetry (DSC) thermograms of the samples (10–20 mg) were re-

corded using a closed-pan type thermal analysis system (model DT-30, Shimadzu) at a sensitivity of ±5 mJ/s, calibration being performed with indium (99.999% purity; melting point, 159 °C; transition energy 21.34 J/g; heating rate, 20 °C/min). Dry nitrogen at a constant flow rate was used as a carrier gas. The heating rate was 10 °C/min throughout unless otherwise stated. Differential thermal analysis (DTA) and thermogravimetry (TG) were also performed using the same system at a sensitivity of ±25 μV and ±5 mg, respectively. The heating rate for DTA ranged from 5 to 20 °C/min and that for TG was the same as that for DSC within the range 30–220 °C, with nitrogen purging being included.

Infrared spectroscopy

Infrared (IR) spectra were registered on a grating infrared spectrophotometer (model 215, Hitachi Co., Japan) using the Nujol mull method. Diffuse reflectance IR spectra of forms (I)–(III) at room and elevated temperatures were determined over the wave number range 700–5000 cm^{-1} on a Fourier transform infrared (FTIR) spectrophotometer (model FTIR-4300, Shimadzu) equipped with a heating apparatus. Samples were dispersed in KBr powder and subjected to analysis.

Elemental analyses

Elemental analyses for all modifications were performed for atoms of C, H and N with a CHN corder (model MT-2, Yanaco) and for S and Cl by the oxygen flask combustion method.

Hot-stage microscopy

The physical and morphological changes undergone by the samples during the process of heating were monitored through microscopy on a Linkam TH-600RH heating stage at a controlled heating rate of 20 °C/min. The major events occurring during the heating process were photographed.

Scanning electron microscopy

Scanning electron photomicrographs of all samples except form (VI) were taken on a scanning electron microscope (JSM-T20, Jeol) at magnifications within the range ×500–×10000.

Evaluation of physicochemical photostability

Three tablets (700 mg each) of diameter 15 mm were prepared for forms (I) and (III), and the two solvates using a single set of flat-faced punches and die, equipped with a compression-tension testing machine. To ensure conformity in the surface conditions of all tablet surfaces, compression was carried out at a constant force of 400 kg. Each tablet was attached to a glass plate with epoxy resin, placed in the rack of a fading tester equipped with a 400 W mercury vapor lamp (Matsuda and Minamida, 1976) and exposed to UV light. Samples were withdrawn from the fading tester at appropriate time intervals for colorimetry; quantitative evaluation of the color changes seen on tablet surfaces before and after irradiation with light was performed on the basis of the Hunter color difference ΔE measured for three tablets with each form of irradiation using an integrating sphere-type color difference meter (model ND-101, Nippon Denshoku) as reported previously (Matsuda et al., 1978); the mean of these determinations was employed. Following this stage, samples were returned to the fading tester, and irradiation continued. In the case of form (II), the powdered sample (100 mg) was fixed on the glass plate for X-ray powder diffractometry and exposed to light, since it shows very poor compressibility which is accompanied by crumbling. This procedure was omitted for the amorphous sample due to low recovery.

Solubility studies

The equilibrium solubility characteristics of five of the modifications, the amorphous form and form (VI) being excluded from this analysis, were investigated in McIlvain buffer solutions of pH 2.2, 3.2, 4.4 and 5.6; an excess of each drug powder (100–1200 mg) was introduced into 250 ml of dissolution medium in a 500 ml Erlenmeyer flask with a glass stopper. The flasks were fixed on the sample holder in a thermostatically maintained water bath (37 ± 0.5 °C) and mechanically shaken at a fixed rate of 89 strokes/min. Aliquots (2 ml) of the solution were withdrawn through a 0.8 μm membrane filter at appropriate time intervals using a syringe and suitably diluted with dissolution medium. Drug concentrations were de-

termined at 228 nm on a UV spectrophotometer. The resultant loss in volume was compensated by addition of dissolution medium maintained at the same temperature.

Results and Discussion

Study on preparing modifications

Recrystallization according to our procedure is performed as given in the particular method chosen among the following: (i) a hot organic solution of the drug is allowed to stand at room temperature ('slow recrystallization'); (ii) rapid cooling of hot organic solutions ('fast recrystallization'); (iii) addition of a small amount of water to hot organic solutions until crystals begin to separate; (iv) addition of solvents other than water to hot DMF or cyclohexanone solutions until separation of the crystals commences; (v) introduction of saturated organic solution into cold water and vigorous stirring; (vi) allowing a saturated solution to stand at room temperature and to undergo evaporation to dryness (slow evaporation); (vii) solvent evaporation-recrystallization in a rotary evaporator under reduced pressure the temperature being varied ('fast evaporation'); (viii) spray drying at three temperatures. Of the above methods, (vi)–(viii) deal with the evaporation of the recrystallization solvent.

A tendency of form (I) to recrystallize from solvents of lower boiling points, as opposed to those boiling at higher temperatures in the case of form (II), was observed for methods (i)–(v) (Table 1). This trend was particularly obvious for method (i) (Fig. 1). Methods (vi) and (vii) also gave results similar to those with the first five, in which the higher the boiling point of solvent used, the greater was the recovery of form (II). In addition, an unstable crystal form (amorphous form) was recrystallized from a very rapid evaporation system (method (viii)). These results strongly suggest that both the boiling point and rate of evaporation of the solvent affect the formation of crystal structure.

X-ray powder diffractometry

Fig. 2 depicts the relative X-ray powder diffraction intensity patterns of all modifications except for the amorphous form. The characteristic angles of diffraction together with the three main peaks for these crystal forms are also listed in Table 2.

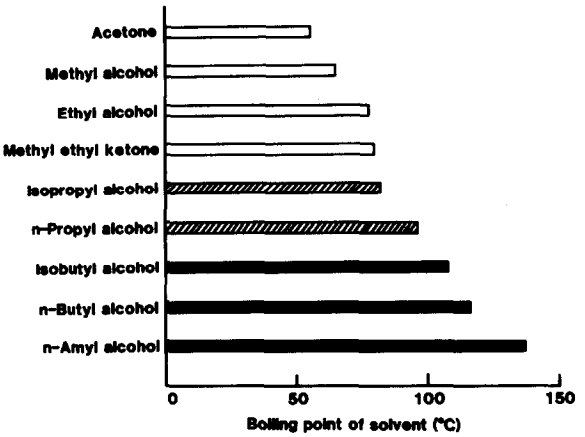

Fig. 1. Crystal forms resulting from the use of various recrystallization solvents (slow recrystallization). (□) form (I), (▨) form (I) + form (II), (■) form (II).

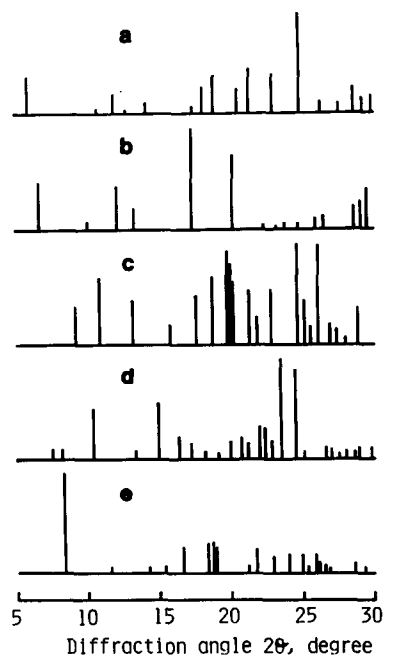

Fig. 2. X-ray powder diffraction patterns of furosemide modifications. (a) Form (I), (b) form (II), (c) form (III), (d) DMF solvate, (e) dioxane solvate.

TABLE 1

Methods of recrystallization and resultant crystal forms (methods (i)–(viii) detailed in the text)

	Solvent	Crystal form			
Method (i)	Acetone	(I)			
	Methyl alcohol	(I)			
	Ethyl alcohol	(I)			
	Methyl ethyl ketone	(I)			
	Isopropyl alcohol	$(I) + (II)_{minor}$			
	n-Propyl alcohol	$(II) + (I)_{minor}$			
	Isobutyl alcohol	(II)			
	n-Butyl alcohol	(II)			
	n-Amyl alcohol	(II)			
	1,4-Dioxane	(V)			
Method (ii)	Isopropyl alcohol	$(I) + (II)_{minor}$			
Method (iii)	Acetone	(I)			
	Methyl alcohol	$(I) + (II)_{minor}$			
	Ethyl alcohol	$(I) + (II)_{minor}$			
	Isopropyl alcohol	$(II) + (I)_{minor}$			
	1,4-Dioxane	(V)			
	N,*N*-Dimethyl formamide	(IV)			
Method (iv)	DMF + methylene chloride	(I)			
	DMF + chloroform	(I)			
	DMF + benzene	(I) + (II)			
	DMF + toluene	(I) + (II)			
	DMF + xylene	(IV)			
	Cyclohexanone + chloroform	(I)			
Method (v)	Acetone	(I)			
	Methyl alcohol	(I)			
Method (vi)	Acetone	(I) + (III)			
	Methyl alcohol	(I) + (II)			
Method (vii)		(Evaporation temperature)			
		0 °C	20 °C	40 °C	60 °C
	Acetone	(III)	(III)	(III)	–
	Methyl alcohol	–	(III)	(III)	(III)
	Ethyl alcohol	–	(III)	(III)	(III)
	Isopropyl alcohol	–	(III)	(III)	(III)
	n-Propyl alcohol	–	–	(III)	(II) + (III)
	Isobutyl alcohol	–	–	–	(II)
	n-Butyl alcohol	–	–	–	(II)
Method (viii)		(Drying temperature)			
		30 °C	70 °C	120 °C	
	Methylene chloride/ methyl alcohol (4 : 1)	Amor.	Amor.	Amor.	
	Chloroform/ methyl alcohol (4 : 1)	Amor.	Amor.	Amor.	
	Chloroform/DMF (4 : 1)	(IV)	(I) + (IV)	(I)	

Amor., amorphous form.

TABLE 2

The three main peaks in X-ray diffraction patterns of furosemide modifications

Modification	2θ (°)	I/I_0 (×100)
Form (I)	24.8	100
	21.3	46
	22.9	40
Form (II)	17.3	100
	20.1	74
	6.7	47
Form (III)	24.6	100
	26.1	98
	19.8	94
DMF solvate	23.5	100
	24.5	90
	14.9	56
Dioxane solvate	8.3	100
	18.7	31
	18.3	29

The amorphous form exhibited no diffraction peak, displaying a halo pattern instead. Distinct differences in X-ray diffraction profiles among the modifications are evident in both Fig. 2 and Table 2. The most significant aspects from comparison of our results with those of Doherty and York (1988) are as follows: The diffraction pattern of form (I) is very similar to that of the untreated commercial sample described by Doherty and York (1988), indicating that it corresponds to their form I. Form (I) obtained via addition of water to acetone, methanol or ethanol in method (iii) is also consistent with form I. The diffraction pattern of form (III) almost coincided with that of form II recrystallized from methanol or ethanol. However, there is no mention in their article of the propanol-recrystallized sample exhibiting another pattern, nor do they define it as the second new crystal form. Form (II) displays a very similar pattern to that of the propanol-recrystallized sample, which thus suggests it to be a novel crystal form. The diffraction patterns of forms (IV) and (V) in the present paper bear no resemblance to those described in their report.

Infrared spectroscopy

Fig. 3 shows the infrared spectra of the modifications as recorded via the Nujol mull technique. Substantial differences are evident among the spectra. In particular, the absorption band in the region 3200–3400 cm^{-1}, as well as that reported by Doherty and York (1988), was characterized fully for individual crystal forms; one can observed correspondence with their results where the secondary amine N-H stretching vibration remains unaltered between forms I and II, the absorption band attributable to this vibration (3370

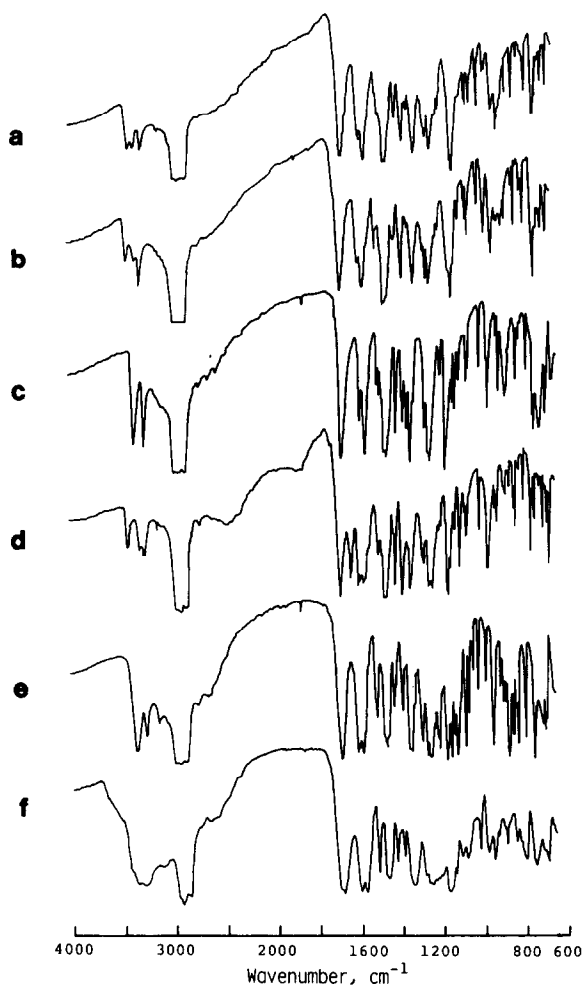

Fig. 3. Infrared spectra of furosemide modifications using the Nujol mull technique. (a) Form (I), (b) form (II), (c) form (III), (d) DMF solvate, (e) dioxane solvate, (f) amorphous form.

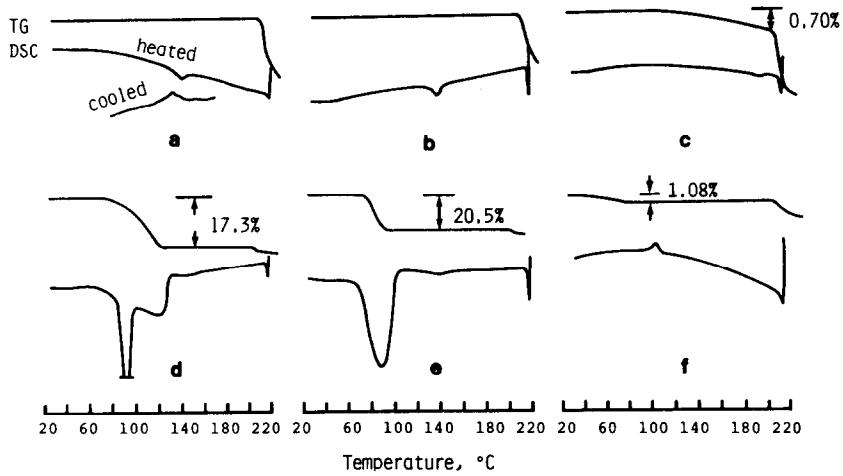

Fig. 4. DSC and TG thermograms of furosemide modifications. (a–f) See Fig. 3.

cm^{-1}) being also in reasonably good agreement for our forms (I) and (III). The apparent lack of an absorption band near 3420 cm^{-1} is also characteristic for form (III). Although Doherty and York described the propanol-recrystallized sample as exhibiting an IR spectrum identical to that of form I, we observed a slight shift in peak position to lower wave number (3350 cm^{-1}), ascribed to the secondary amine N-H vibration (3370 cm^{-1}), for form (II).

Forms (IV) and (V) exhibit absorption peaks at 1650 and near 1100 cm^{-1}, attributable to –CO–N< of DMF and C–O–C of 1,4-dioxane, respectively, indicative of their presence as solvates. The absorption spectrum of the amorphous form was broad throughout the entire range of wave numbers as a consequence of possessing a low degree of crystallinity. A more detailed discussion of the IR spectra including FTIR will be presented in a forthcoming paper on the structural analysis of crystals of two polymorphs (forms (I) and (II)) of the drug.

Thermal analysis

Fig. 4 shows DSC and TG thermograms of six modifications. The DSC curve for form (I) shows a weak endotherm at 138.0–142.0 °C similar to the result for form I, and a melting endotherm at 217.0 °C before decomposition. The TG curve shows no change over the temperature range studied, suggesting that the first endotherm does not arise from desolvation. An exotherm occurs at about 136 °C, close to the endothermic temperature for initial heating to 180 °C and subsequent cooling. This finding concerning the heating-cooling cycle was also observed under various conditions of heating and cooling rates. The X-ray diffraction pattern of the sample after cooling agrees well with that of intact form (I). These results suggest that enantiotropism (Kato and Kido, 1977; Miyoshi et al., 1979; Brandstätter and Wurian, 1982; Brandstätter et al., 1982a,b; Shah and Britten, 1987) exists between form (I) (low-temperature-stable form) and a new, higher-temperature-stable form.

The DSC curve for form (II) shows a weak endotherm at 137.0–140.0 °C and a melting endotherm at 217.0 °C as occurs for form (I) as well. The TG curve demonstrates that no weight loss took place due to desolvation. The exotherm during the cooling process was observed at about 136 °C, similar to the case for form (I). The sample after cooling was also identical with form (I) as judged on the basis of the X-ray powder diffraction pattern.

In contrast to form II for which the first endotherm was lacking, the DSC curve of form (III) shows a weak endotherm at 184.0–196.0 °C and a subsequent melting endotherm at 213.0–219.0 °C. Interestingly, the TG curve indicates that a grad-

TABLE 3

Elemental analyses of furosemide modifications

Modification	Formula	Elemental analysis (%): Calcd. (Found)					Solvent (%)	
		C	H	N	S	Cl	Calcd.	Found [a]
Form (I)	$C_{12}H_{11}ClN_2O_5S$	43.54	3.33	8.47	9.68	10.58	0	–
		(43.56	3.23	8.19	9.84	10.57)		
Form (II)	$C_{12}H_{11}ClN_2O_5S$	43.54	3.33	8.47	9.68	10.58	0	–
		(43.52	3.26	8.32	9.84	10.74)		
Form (III)	$C_{12}H_{11}ClN_2O_5S$	43.54	3.33	8.47	9.68	10.58	0	0.68–
		(43.75	3.28	8.29	9.95	10.66)		0.98
DMF solvate	$C_{12}H_{11}ClN_2O_5S \cdot C_3H_7NO$	44.57 (45.34	4.46 4.46	10.40 10.48	7.92 8.20	8.67 8.94)	18.10	17.3
Dioxane solvate	$C_{12}H_{11}ClN_2O_5S \cdot C_4H_8O_2$	45.84 (45.56	4.54 4.41	6.68 6.63	7.64 7.81	8.30 8.43)	21.03	20.5
Amorphous form	$C_{12}H_{11}ClN_2O_5S$	43.54	3.33	8.47	9.68	10.58	0	1.08
		(43.28	3.50	7.97	9.76	10.29)		

[a] Thermogravimetry.

ual weight loss of only about 0.70% of the total occurs within the range 100–200 °C, while the authors of the preceding paper detected no weight loss at all. Nevertheless, the X-ray powder diffraction pattern of this crystal form observed before and after removal of the recrystallization solvent shows that no significant change occurs. The data indicate that acetone was present in crystals of form (III) at a ratio of 1 mol acetone per 25 mol crystal. Based on this value, the molecules of acetone are presumably entrapped nonstoichiometrically and dispersed around that portion of the crystal which has a lattice defect, and thus no correlation with crystal structure is found. Such characteristically low weight loss at higher temperatures also suggests that acetone molecules are not readily released after being entrapped in the crystal form. This inference is supported by the fact that even under severe conditions (65 °C, 10^{-3} Torr, 16.5 h), complete desolvation is not attainable. As occurs with forms (I) and (II), an exotherm is found at 132.6 °C during the process of cooling of a sample previously heated to 190 °C. The X-ray powder diffraction pattern of the sample after cooling to room temperature is consistent with that of intact form (I). These findings led to the conclusion that each of the forms (I)–(III) undergoes transformation to a higher-temperature-stable form on heating and proceeds along a common reverse pathway to recover form (I) on cooling. Doherty and York (1988) were unable to detect changes in the thermograms for reheating of a cooled sample of form II. Based on our results, where the temperature of the first endotherm of form (III) is much higher than that of form (I), we believe that they probably would have observed the initial endothermic peak at approx. 140 °C, corresponding to that of form (I), if they had firstly reheated the sample to about 200 °C, which lies below the melting point, and then carried out cooling.

The DSC curve of form (IV) shows a sharp endothermic peak at 92.5 °C, accompanied by a shoulder at 102.0 °C, and followed by a slight endotherm at 143.0 °C. The TG curve represents a loss of 17.3% of the total weight at 70.0–127.0 °C corresponding to the first endotherm, suggesting desolvation to be the cause. This value is very close to that of 18.1% determined theoretically for a 1 : 1 DMF solvate. The results of the elemental analyses (Table 3) are also in support of the formation of solvate with DMF. The X-ray powder

diffraction pattern of a desolvated sample that was heated once to the temperature at which weight loss occurred and then cooled revealed it to be identical with form (I). The second endotherm at 143.0 °C was therefore attributable to that of the resultant form (I) undergoing transformation to a higher-temperature-stable form.

The DSC curve for form (V) displays the strong and weak endothermic peaks at 89.0 and 139.0 °C, respectively, with the final melting endotherm being at 218.0 °C. A 20.5% loss in total weight indicated by the TG curve suggests that the endothermic peak at 89.0 °C is caused by desolvation, thereby demonstrating the close agreement between the observed and theoretical values for a 1 : 1 dioxane solvate. The results of elemental analyses and X-ray powder diffractometry demonstrate that form (V) is also a solvate with dioxane and is transformed into form (I) by desolvation at temperatures above approx. 90 °C. The weak endotherm at 139.0 °C, corresponding to the endothermic peak for form (I), is indicative of the transformation of form (I) into a higher-temperature-stable form. An exotherm was also observed at about 130 °C. Henceforth, forms (IV) and (V) will be referred to as DMF and dioxane solvates, respectively.

The DSC curve for the amorphous form has an exothermic peak at 103.0–104.0 °C arising from the transformation to a crystalline form, and a melting endotherm at 214.0–215.0 °C. We were unable to examine the crystalline state of the sample by X-ray powder diffractometry above the exothermic temperature due to the low yield. The existence of an endothermic peak correlated with the transformation to a higher-temperature-stable form, as observed for all the other forms, and of enantiotropism was not established. This may be due to the low degree of crystallinity of the resultant form after crystallization. In contrast to form (III), a weight loss of 1.08% of the total due to desolvation was determined at lower temperatures ranging from room temperature to 76 °C. The explanation for this observation is probably that the crystal structure has a tendency to release entrapped solvent molecules as a result of the looser crystal packing compared to form (III).

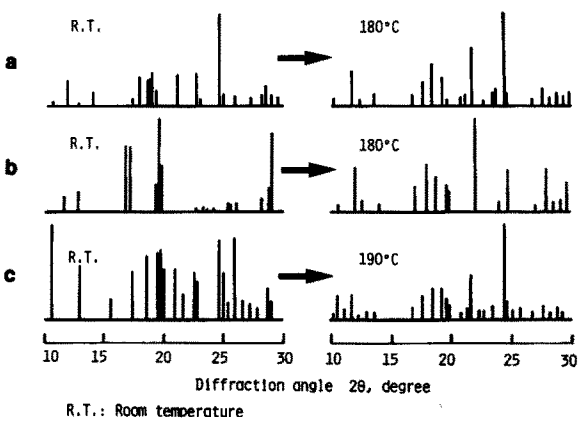

Fig. 5. Changes in X-ray powder diffraction patterns of forms (I)–(III) on transformation to form (VI) at high temperatures. (a) Form (I), (b) form (II), (c) form (III).

Crystal form at high temperature

In order to confirm the existence of a crystal form at high temperatures, X-ray powder diffraction patterns were recorded for forms (I)–(III) at room and elevated temperatures, corresponding to a temperature intermediate between that of the transformation to the higher-temperature-stable form and the melting point (for forms (I) and (II): 180 °C; for form (III): 190 °C) (Fig. 5). The patterns at high temperatures differ markedly from those of all other forms, but almost coincide with each other, suggesting that they possess an identical crystal structure. This crystal sample is henceforth denoted form (VI).

FTIR spectra were also obtained under thermal conditions identical to those for X-ray powder diffractometry (Fig. 6). In contrast to the report by Doherty and York (1988) that form I revealed no significant shift in the vibrational portions of the principal functional group (VT-FTIR), the spectra of samples registered after heating crystals of forms (I) and (II) to 180 °C coincided well, differing from those of the intact crystal forms at room temperature. The spectrum of form (VI) was generally broader than those of intact forms (I) and (II), and the shift in position of the absorption band at approx. 3300 cm^{-1} attributable to secondary amine N-H stretching vibration was particularly large, typical of the absorption properties of form (VI). Although an exception was

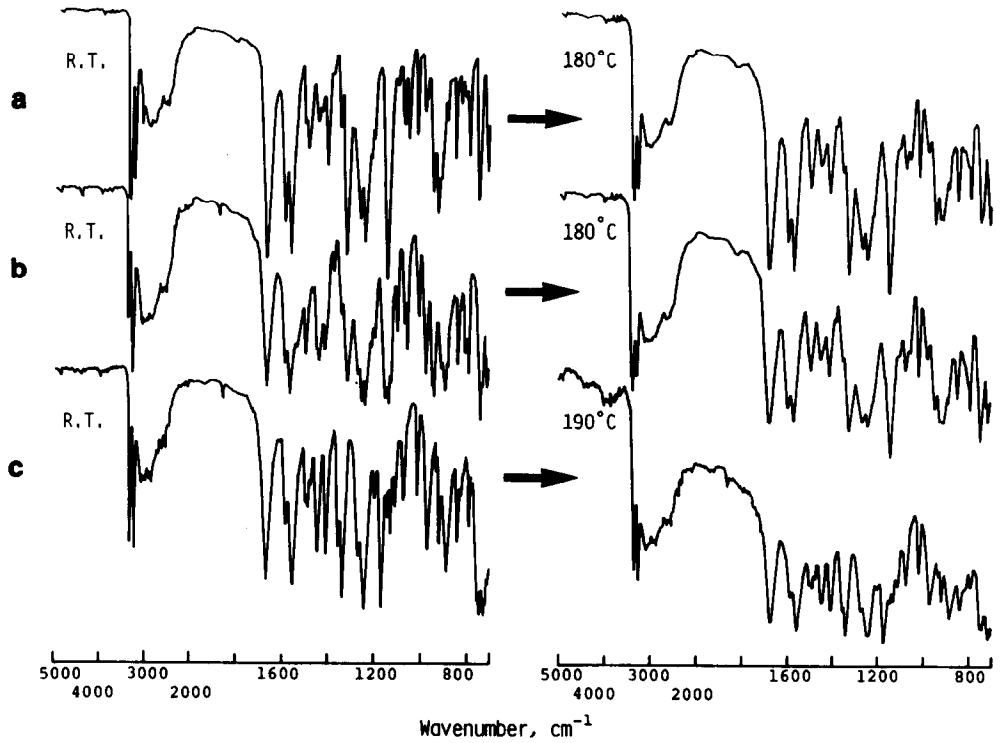

Fig. 6. Changes in FTIR spectra of forms (I)–(III) at high temperatures. (a) Form (I), (b) form (II), (c) form (III).

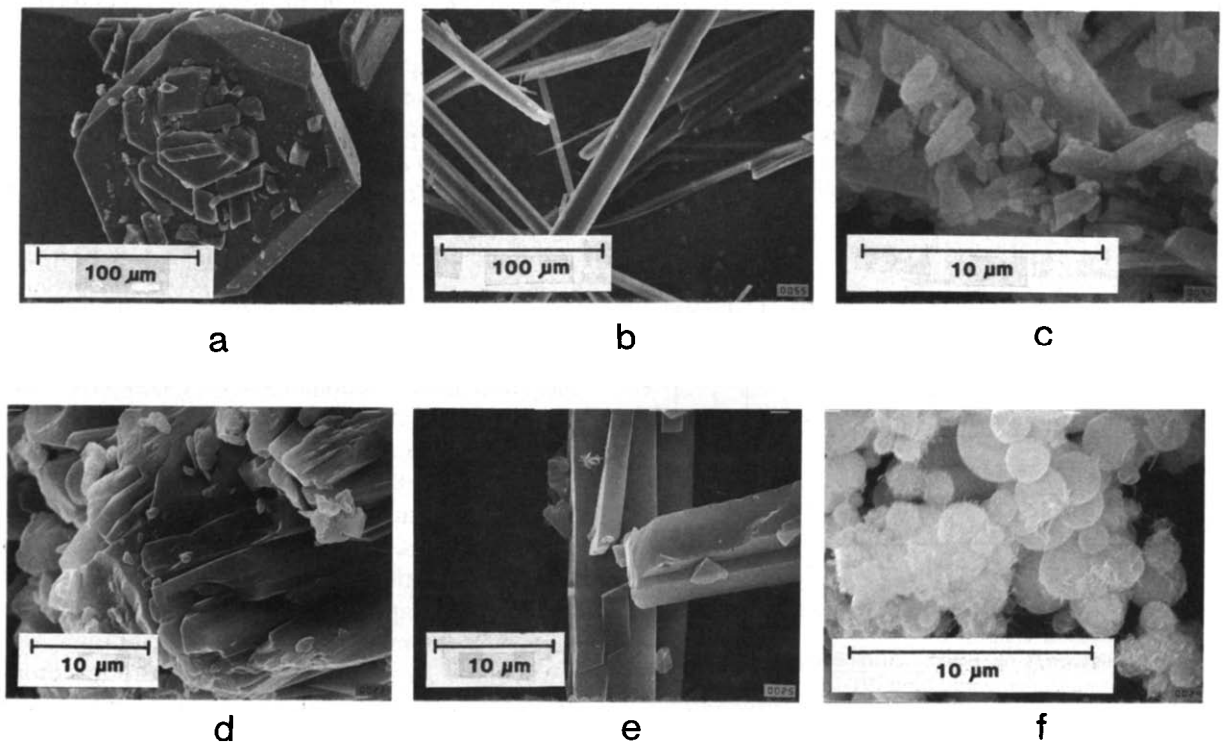

Fig. 7. Scanning electron photomicrographs of furosemide modifications. (a–f) See Fig. 3.

noted to the generally observed close agreement between the spectrum of form (III) at high temperature and those of forms (I) and (II) for the case of its incomplete transformation to form (VI), a significant change corresponding to the results obtained for the X-ray powder diffraction profile shown in Fig. 5 was also demonstrable for form (III), at variance with form II of Doherty and York. Figs 5 and 6 show that conformational changes in the crystal packing of molecules occur in each of these forms when the endothermic temperature is exceeded.

Morphological characterization

Fig. 7 shows scanning electron photomicrographs illustrating the crystals formed by the various modifications except for form (VI). Distinct morphological differences were evident among these samples. Form (I) gave rise to the largest crystals, which appear as hexagonal tabular crystals. Form (II) recrystallized in the form of longer needles, whereas form (III) resulted in fine prisms with a small extent of elongation. Even at magnifications above $\times 35\,000$, no appreciable surface change for crystals of form (III) was detected after desolvation. The DMF solvate formed polycrystals with rounded edges, composed of acicular crystals, while the dioxane solvate comprised sharp-edged crystals. In contrast, the amorphous form recrystallized as minute and spherical crystals forming agglomerates resembling a bunch of grapes. Such characteristic crystal morphology is very similar to that reported previously for the amorphous form of novobiocin (Mullins and Macek, 1960). The needle-like crystals that protrude from the surface of the crystal are probably the 'whiskers' resulting from transformation to form (I).

Fig. 8 depicts morphological changes in crystals of form (II) on passing the temperature of the first endotherm under a hot-stage microscope. The solid-state transformation that accompanies the breaking up and bending of crystals as reported by Doherty and York (1988), although no photograph was presented in their paper, could also be clearly recognized as indicated in fig. 8 by arrows. This phenomenon may be caused by mechanical stress arising from the rearrangement of molecules

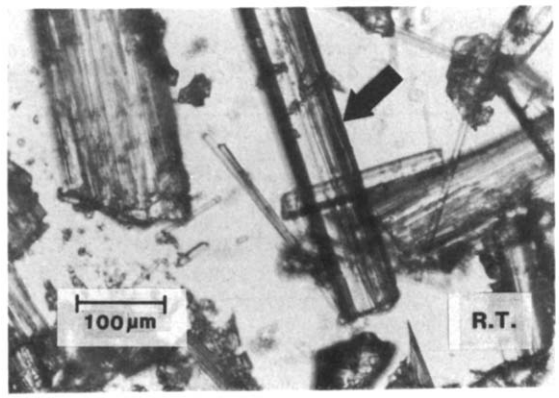

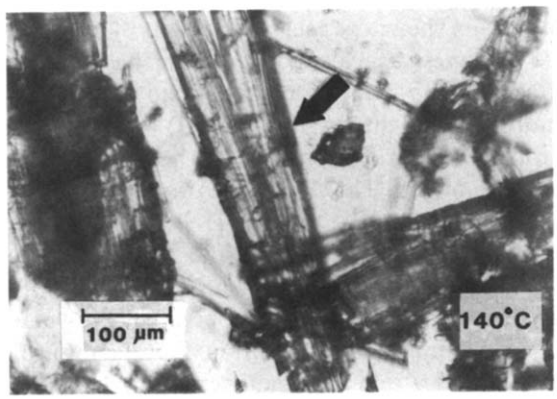

Fig. 8. Solid-state polymorphic transformation of form (II) to form (VI) under hot-stage microscopy.

within the crystal lattice. Although they described the transformation of form I, we observed no evidence of morphological change for forms (I) and (III). The fact that the alteration is observed only for form (II) crystals may be related to the higher activation energy of its transformation to form (VI), as discussed below.

Thermodynamic stability of polymorphic forms (I)–(III) and (VI)

To evaluate the thermodynamic stability of the crystal forms, the activation energy for polymorphic transformation to form (VI) for each of the forms (I)–(III) was calculated according to Kissinger's method (Kissinger, 1957) using the data obtained via DTA (Table 4). The heat of transfor-

TABLE 4

Activation energy for polymorphic transformation (E_a) and heat of transformation (ΔH) for forms (I)–(III) and (VI)

Transformation system	E_a (kJ/mol)	ΔH (kJ/mol) ± S.D. ($n = 3$)
(I) → (VI)	9.69×10^2	2.66 ± 0.12
(II) → (VI)	2.34×10^3	2.04 ± 0.10
(III) → (VI)	2.46×10^2	1.15 ± 0.07
(VI) → (I)	– [a]	2.59 ± 0.02

[a] E_a could not be evaluated.

mation (ΔH) was also determined from the area of the endotherm or exotherm on DSC thermograms (heating rate 20 °C/min). Fig. 9 shows Kissinger plots for the above polymorphs. Good linearity is shown by each of the plots. The activation energies, as calculated on the basis of the slopes of the regression lines, had magnitudes conforming to the order, form (II) > form (I) > form (III), the value for form (II) being far greater than the others. The ΔH values for the transformations (I) → (VI) and (VI) → (I) were determined to be approx. 2.7 and 2.6 kJ/mol, respectively, their close agreement therefore verifying the existence of enantiotropism. These values do not significantly differ from those for form I (first run, $\Delta H = 2.2$ kJ/mol; reheating, $\Delta H = 2.1$ kJ/mol) and those obtained for the other enantiotropic transformation systems (Burger and Ramberger, 1979). The thermodynamic stability of forms (II), (III) and (VI) relative to the energy

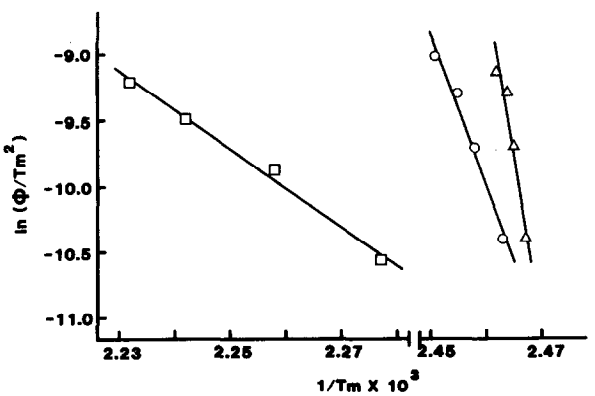

Fig. 9. Kissinger plots for polymorphic transformations of forms (I)–(III) to form (VI). (○) form (I), (△) form (II), (□) form (III). Sample weight: 10 ± 0.1 mg.

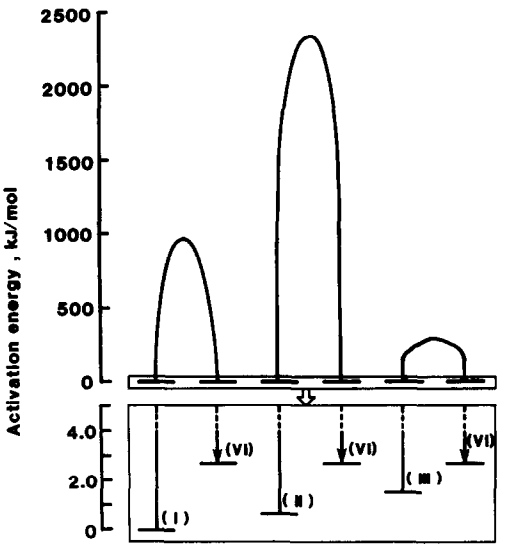

Fig. 10. Schematic diagram of activation energies for polymorphic transformations of forms (I)–(III) to form (VI), and their energy levels relative to that of form (I) as a standard.

level of form (I) as a standard can therefore be depicted in the manner shown in Fig. 10 using the values of E_a and ΔH. Fig. 10 clearly demonstrates that form (I) is a stable form at low temperature, and that forms (II) and (III) are metastable types.

The mutual transformations corresponding to the seven modifications investigated are illustrated in Fig. 11. Forms (II), (III) and the amorphous form each underwent transformation to form (I) at high humidities, as indicated by the dashed lines.

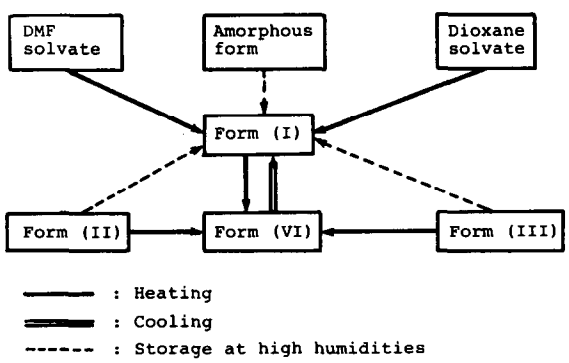

Fig. 11. Mutual transformation of furosemide modifications under various stress conditions.

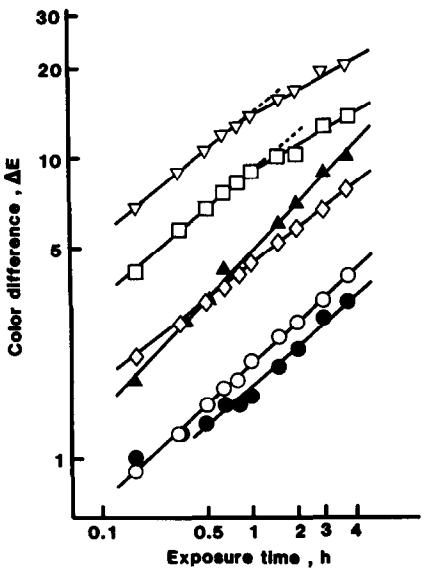

Fig. 12. Double-logarithmic plots for coloration process of furosemide modifications under irradiation by a mercury vapor lamp. Tablet: (○) form (I), (□) form (III), (▽) DMF solvate, (◇) dioxane solvate. Powder: (●) form (I), (▲) form (II).

Physicochemical photostability

According to the Pharmacopeia of Japan (JP XI, 1986), furosemide undergoes gradual coloration upon exposure to light and is recommended to be protected from light. Several reports have appeared concerning photolytic degradation of this drug in either aqueous or organic solvents (Rowbotham et al., 1976; Moore and Tamat, 1980; Moore and Sithipitaks, 1983; Neil et al., 1984). A matter of importance from the viewpoint of pharmaceutics is the quantitative evaluation of the photostability of these crystal forms.

Assuming that the progress of darkening, as determined on the basis of the color difference, ΔE, obeys the following kinetic equation, a linear plot with a slope of $1/(1-n)$ should result for the relationship between ΔE and t on a double-logarithmic scale (Matsuda and Masahara, 1983):

$$\frac{d\Delta E}{dt} = k(\Delta E)^n \tag{1}$$

where t and k represent the irradiation time and color-darkening rate constant, respectively, with n being a constant.

Fig. 12 shows double-logarithmic plots for forms (I)–(III) and the two solvates. Excellent linearity is shown in the plots for all crystal forms. The n values are almost equal among samples (range: -1.2 for form (I) to -1.6 for the DMF

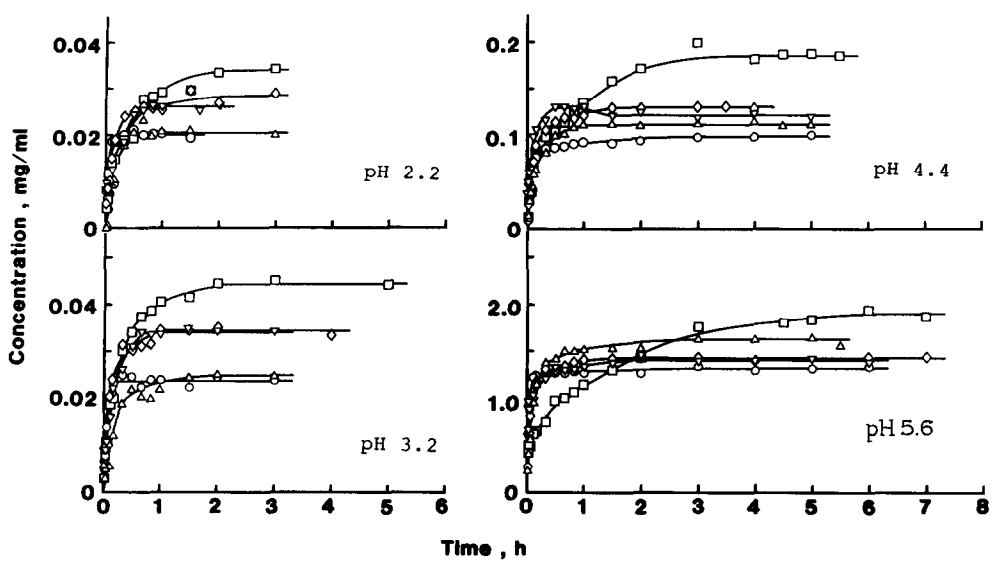

Fig. 13. Dissolution profiles of furosemide modifications in buffer solution at various pH values at 37°C. (○) Form (I), (△) form (II), (□) form (III), (▽) DMF solvate, (◇) dioxane solvate.

solvate) except for the powder sample of form (II), suggesting that the coloration processes follow apparently identical kinetics. Interestingly, striking differences in the degree of coloration were observed among the three polymorphs; although forms (II) and (III) are very susceptible to coloration even after short-term irradiation, the value of ΔE for form (I) remained less than 3 NBS units, corresponding visually to only 'noticeable', regardless of the condition of the sample after prolonged irradiation (2 h). This result demonstrates that form (I) is sufficiently stable against light. Examples of solid-state photochemical reactions for polymorphic drugs are less well understood (Schmidt, 1964, 1971) and it remains unclear as to whether the difference in coloration is correlated with the extent of chemical stability of furosemide.

Equilibrium solubility

Since furosemide is a weakly acidic drug, its solubility is dependent on the pH of the dissolution medium. Fig. 13 shows dissolution profiles for the three polymorphs and two solvates in buffer solutions of various pH values. Equilibrium solubility is attained within 1 h except for form (III) and increases with rise in pH without altering the conformity with the order of magnitude among modifications. No polymorphic transformations of forms (II) and (III) occurred even after a long-term run. The means of the solubility ratios of forms (II) and (III), and DMF and dioxane solvates to that of form (I) measured at the given pH values were 1.11, 1.72, 1.26 and 1.32, respectively. The highest value was obtained for form (III) and was very close to that (1.63) reported by Doherty and York (1988). However, a more accurate approach to the exact comparison of dissolution properties for crystal forms is provided by the evaluation of intrinsic solubility independently of the pH.

The relationship between the equilibrium solubility and pH is expressed by the following equation (Aulton, 1988):

$$S_t = S_o(1 + 10^{(pH - pK_a)}) \quad (2)$$

where S_t denotes the overall solubility of the drug and S_o is the solubility of its unionized form. The

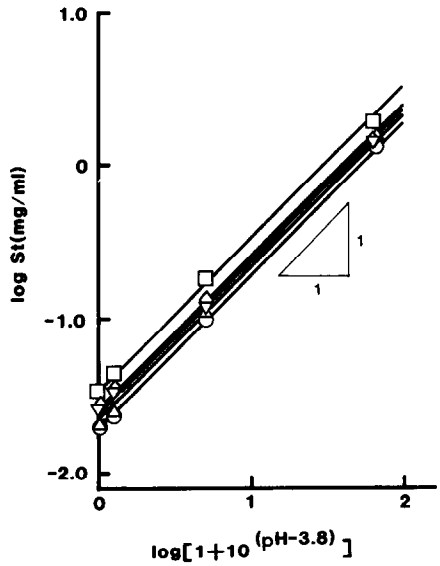

Fig. 14. Relationship between overall solubility (S_t) and pH. Symbols: as given in Fig. 13.

mean pK_a value (3.80 ± 0.15; $n = 30$) of every crystal form as determined from Eqn 2 using S_t measured at two different pH levels was almost identical to that (3.9) reported by Neil et al. (1984). Eqn 2 indicates that the relationship demonstrated on plotting S_t as a function of $(1 + 10^{(pH-3.8)})$ using a double-logarithmic scale should be linear and have a slope of unity. The data shown in Fig. 14 confirm the validity of this relationship for all crystal forms. Thus, we can obtain S_o from the intercept of the regression line with the ordinate (Table 5). The order of magnitude for S_o was quite consistent with that for S_t, indicating the greater solubility of form (III) which

TABLE 5

Solubility properties and free energy difference of modifications

Modification	$(S_t)_{5.6}/(S_t)_{2.2}^{a}$	S_o (μg/ml)	ΔG (cal/mol)
Form (I)	65.8	19.8	–
Form (II)	80.3	21.8	−63.2
Form (III)	56.2	33.8	−332.2
DMF solvate	54.4	24.7	−138.1
Dioxane solvate	50.4	25.9	−167.4

[a] Ratio of overall solubility at pH 5.6 to that at pH 2.2.

also amounted to a value 1.71-fold greater than that of form (I). This can be clearly explained on comparing the highest crystal energy level of form (III) among the polymorphs shown in Fig. 10.

The free energy difference ΔG between forms (III) and (I) at a particular temperature (37.0 °C) was calculated by using Eqn 3 (Aguiar and Zelmer, 1969):

$$\Delta G = RT\frac{S_{o(III)}}{S_{o(I)}} \quad (3)$$

Although the value (−332 cal/mol) determined for this system was not comparable to that (−774 cal/mol) between the chloramphenicol palmitate polymorphs, it was in reasonable agreement with that (−291 cal/mol) for the sulfameter polymorphs which exhibited a significant difference in bioavailability following oral administration (Khalil et al., 1972). The crystals of form (III) may be expected to display superior gastrointestinal absorption properties to the commercially available form (I).

References

Aguiar, A.J. and Zelmer, J.E., Dissolution behavior of polymorphs of chloramphenicol palmitate and mefenamic acid. *J. Pharm. Sci.*, 58 (1969) 983–987.

Aulton, M.E., *Pharmaceutics, The Science of Dosage Form Design*, Churchill, Edinburgh, 1988, p. 72.

K.-Brandstätter, M. and Wurian, I., Thermoanalytische und IR-spektroskopische Untersuchungen an enantiotrop polymorphen Arzneistoffen. 1. Mitteilung. *Sci. Pharm.*, 50 (1982) 3–11.

K.-Brandstätter, M., Wurian, I. and Geiler, M., Thermoanalytische und IR-spektroskopische Untersuchungen an enantiotrop polymorphen Arzneistoffen. 2. Mitteilung. *Sci. Pharm.*, 50 (1982a) 91–98.

K.-Brandstätter, M., Wurian, I. and Geiler, M., Thermoanalytische und IR-spektroskopische Untersuchungen an enantiotrop polymorphen Arzneistoffen. 3. Mitteilung. *Sci. Pharm.*, 50 (1982b) 208–216.

Burger, A. and Ramberger, R., On the polymorphism of pharmaceuticals and other molecular crystals. II. *Mikrochim. Acta*, (1979) 273–316.

Doherty, C. and York, P., Mechanisms of dissolution of frusemide/PVP solid dispersions. *Int. J. Pharm.*, 34 (1987a) 197–205.

Doherty, C. and York, P., Evidence for solid- and liquid-state interactions in a furosemide-polyvinylpyrrolidone solid dispersion. *J. Pharm. Sci.*, 76 (1987b) 731–737.

Doherty, C. and York, P., Frusemide crystal forms; solid state and physicochemical analyses. *Int. J. Pharm.*, 47 (1988) 141–155.

Dubios, J.L. and Ford, J.L., Similarities in the release rates of different drugs from polyethylene glycol 6000 solid dispersions. *J. Pharm. Pharmacol.*, 37 (1985) 494–496.

Hasegawa, A., Kawamura, R., Nakagawa, H. and Sugimoto, I., Physical properties of solid dispersions of poorly water-soluble drugs with enteric coating agents. *Chem. Pharm. Bull.*, 33 (1985) 3429–3435.

Kato, Y. and Kido, K., Polymorphism of homosulfamine and the stability of its hydrate. *Yakugaku Zasshi*, 97 (1977) 1111–1116.

Khalil, S.A., Moustafa, M.A., Ebian, A.R. and Motawi, M.M., GI absorption of two crystal forms of sulfameter in man. *J. Pharm. Sci.*, 61 (1972) 1615–1617.

Kingsford, M., Eggers, N.J., Soteros, G., Maling, T.J.B. and Shirkey, R.J., An in-vivo–in-vitro correlation for the bioavailability of frusemide tablets. *J. Pharm. Pharmacol.*, 36 (1984) 536–538.

Kissinger, H.E., Reaction kinetics in differential thermal analysis. *Anal. Chem.*, 29 (1957) 1702–1706.

Matsuda, Y. and Minamida, Y., Stability of solid dosage forms: Coloration and photolytic degradation of sulfisomidine tablets by exaggerated ultraviolet irradiation. *Chem. Pharm. Bull.*, 24 (1976) 2229–2236.

Matsuda, Y., Inouye, H. and Nakanishi, R., Stabilization of sulfisomidine tablets by use of film coating containing UV absorber: Protection of coloration and photolytic degradation from exaggerated light. *J. Pharm. Sci.*, 67 (1978) 196–201.

Matsuda, Y. and Masahara, R., Photostability of solid-state ubidecarenone at ordinary and elevated temperatures under exaggerated UV irradiation. *J. Pharm. Sci.*, 72 (1983) 1198–1203.

Matsuda, Y. and Tatsumi, E., Physicochemical characterization of furosemide polymorphs and evaluation of their stability against some environmental factors. *J. Pharmacobio-Dyn.*, 12 (1989) s-38.

McNamara, P.J., Foster, T.S. and Digenis, G.A., Influence of tablet dissolution on furosemide bioavailability: A bioequivalence study. *Pharm. Res.*, 4 (1987) 150–153.

Miyoshi, F., Tokuno, K., Watanabe, T., Matsui, M. and Ohashi, T., Organic sulfur compounds. IV. The phase transition of 1-methyl-thiolanium iodide. *Yakugaku Zasshi*, 99 (1979) 924–928.

Moore, D.E. and Tamat, S.R., Photosensitization by drugs: photolysis of some chlorine-containing drugs. *J. Pharm. Pharmacol.*, 32 (1980) 172–177.

Moore, D.E. and Sithipitaks, V., Photolytic degradation of frusemide. *J. Pharm. Pharmacol.*, 35 (1983) 489–493.

Mullins, J.D. and Macek, T.J., Some pharmaceutical properties of novobiocin. *J. Am. Pharm. Assoc.*, 49 (1960) 245–248.

Neil, J.M., Fell, A.F. and Smith, G., Evaluation of the stability of frusemide in intravenous infusions by reversed phase

high-performance liquid chromatography. *Int. J. Pharm.*, 22 (1984) 105–126.

Rowbotham, P.C., Stanford, J.B. and Sugden, J.K., Some aspects of the photochemical degradation of frusemide. *Pharm. Acta Helv.*, 51 (1976) 304–307.

Schmidt, G.M.J., Topochemistry. III. The crystal chemistry of some *trans*-cinnamic acids. *J. Chem. Soc.*, 1964 (1964) 2014–2021.

Schmidt, G.M.J., Photodimerization in the solid state. *Pure Appl. Chem.*, 27 (1971) 647–678.

Shah, A.C. and Britten, N.J., Evaluation of reversible polymorphic phase transitions by thermal analysis. *J. Pharm. Pharmacol.*, 39 (1987) 736–738.